Proceedings of the 2009 IEEE International Conference on Systems, Man, and Cybernetics
San Antonio, TX, USA - October 2009

A Shadow Detection Method for Remote Sensing Images Using Affinity Propagation Algorithm

Huaiying Xia[1], Xinyu Chen[1]
[1]Image Processing and Pattern Recognition Laboratory
Beijing Normal University
Beijing, 100875, China
xia_huaiying@163.com, xychen@bnu.edu.cn

Ping Guo[1, 2]
[2]School of Computer Science and Technology
Beijing Institute of Technology
Beijing, 100081, China
pguo@ieee.org

Abstract—**Shadow detection in high spatial resolution remote sensing image is very critical for locating geographical targets. In this paper, we proposed a new shadow detection method using Affinity Propagation (AP) algorithm in the Hue-Saturation–Intensity (HSI) color space. Because the pixel matrix is a large-scale matrix, if we apply AP algorithm directly on the raw pixel space, it will be computation intensive to calculate the similarity matrix. To solve this problem, we propose to divide the matrix into several blocks and then applying AP to detect shadows in H, S and I components respectively. Then, three detected images are fused to obtain a final shadow detection result. Comparative experiments are performed for *K*-means and threshold segmentation methods. The experimental results show that higher detection accuracy of the proposed approach is obtained, and it can solve the problems of false dismissals of *K*-means and threshold segmentation method.**

***Keywords*—Affinity Propagation, Shadow Detection, Remote Sensing Image, HSI Color Space, *K*-means**

I. INTRODUCTION

In high spatial resolution remote sensing images, shadows are usually cast by elevated objects such as buildings, bridges, and towers, which is especially obvious in urban regions. Shadows can provide geometric and semantic information contained in images, including cues about shapes and relative positions of objects, as well as the characteristics of surfaces and light sources. However, shadows may also cause loss of feature information, false color tone, and objects' shape distortions, which affect the quality of images seriously, and influence the effects of image processing directly, such as object recognition, change detection and scene matching [1] [2] [3]. Hence, it is important to segment shadow regions and restore their information for image interpretation.

To process shadows or to use the information provided by shadows, we must detect shadows accurately first. It is not difficult for humans to identify shadow in remote sensing images, because shadow itself is one of the fundamental elements in visual photo interpretation for obtaining information about the shape, relative position, and surface characteristics of objects in the scene. However, identifying shadows in digital images by computers involves developing effective algorithms in solving many difficult problems.

Many techniques for shadow detection are developed for video images. However, in remote sensing images field, few techniques are developed, which mainly based on model and property [2]. The approach based on model employs *a priori* knowledge of the illumination and the 3D geometry of the scene being imaged to calculate positions of shadows. However, this method has rarely been used because the prior knowledge is not always available. The method based on property is generally used by analysis of lightness, geometry structure and color character [3]. Recent existing shadow detection methods are commonly based on property, which can be summarized into three types: threshold segmentation method, color space ratios and photometric color invariants, and homomorphic filtering [1] [3]. Those methods get some achievements. However, none of them alone achieves common acceptability to all kinds of images. The main reason is the complexity of image shadow formation mechanism. Shadow areas are believed to be of lower intensity than surrounding areas. For gray images, shadows could be detected by appropriate intensity threshold. However, for color images, there exist no-shadowed areas with low intensity (e.g. areas with darker colors), threshold techniques, such as histogram threshold method, Otsu's method, maximum entropy threshold, may misclassify these areas as shadows [4] [5]. To overcome this drawback, we propose a novel method based on the Affinity Propagation (AP) clustering algorithm in the HSI color space for shadow detection. Comparative experiments are performed for *K*-means [6] and histogram threshold methods [7]. These methods are comparable because they are actually image segmentation method. Experimental results show that the proposed method is better than *K*-means and histogram threshold in terms of accuracy, stability and robustness.

This paper is organized as follows: In Section II, the AP clustering method and HSI color space are reviewed. Section III presents the developed shadow detection approach. In Section IV, experimental results are presented and analyzed. And finally, some discussions and conclusions are given in Section V.

II. RELATED WORK

A. Affinity Propagation

The AP clustering technique was presented by Brendan J. Frey and Delbert Dueck [8]. AP clustering begins with a collection of real-valued similarities between pairs of data points, and iteratively exchanges the real-valued messages between data points so as to produce a high-quality set of centers and corresponding clusters. There are several indicators in AP.

The similarity $s(i, k)$ indicates how well the data point with index k is suitable to be the center for data point i. The similarity is the negative squared error for minimizing the squared error, thus for points x_i and x_k,

$$s(i,k) = -\left\| x_i - x_k \right\|^2 . \quad (1)$$

When the value of $s(i, k)$ is infinite (INF), messages will not be exchanged between points x_i and x_k. In particular, a real number $s(k, k)$ for each data point k is assigned a common value so that data points with larger values of $s(k, k)$ are more likely to be chosen as centers after the message-passing procedure. These values are referred to as "preferences", which directly decides the number of clusters. The bigger number of clusters is, the larger values of the input preferences are.

There are two kinds of message exchanged between data points, the first one is the "responsibility" $r(i, k)$, which is sent from data point i to point k, reflecting the accumulated evidence for how well-suited point k is to serve as the center for point i, considering other potential centers for point i. In particular, the "self-responsibility" reflects accumulated evidence that point k is a center, based on its input preference tempered by how ill-suited it is to be assigned to another center. The second one is the "availability" $a(i, k)$, which is sent from candidate center point k to point i, reflecting the accumulated evidence for how appropriate it would be for point i to choose point k as its center, considering the support from other point that point k should be a center. In particular, the "self-availability" a(k, k) reflects accumulated evidence that point k is a center, based on the positive responsibilities sent to candidate center k from other points.

The whole clustering procedure can be divided into the following steps:

1) The availabilities are initialized to zero: $a(i, k) = 0$. The similarity is computed and $s(k, k)$ is assigned a common value based on the dataset's value range. In our experiment, we initialize $s(k, k)$ to be the minimum of input similarities.

2) The responsibilities are computed using the rule (*2*),

$$r(i,k) \leftarrow s(i,k) - \max_{k':k' \neq k} \{a(i,k') + s(i,k')\} . \quad (2)$$

3) The availabilities are computed using the rule (*3*),

$$a(i,k) \leftarrow \min\{0, r(k,k) + \sum_{i':i' \notin \{i,k\}} \max\{0, r(i',k)\}\} . \quad (3)$$

4) The self-availability $a(k, k)$ *is updated differently*:

$$a(k,k) \leftarrow \sum_{i':i' \neq k} \max\{0, r(i',k)\} . \quad (4)$$

5) If any of the following situations occurs: after a fixed number of iterations, after changes in the messages fall below a threshold, or after the local decisions stay constant for some number of iterations, the clustering procedure is terminated, else go to step 2.

6) Determine the center and their points. For point i, the value of k that maximizes $a(i, k) + r(i, k)$ either identifies point i as a center if $k = i$, or identifies the data point that is the center for point i.

In order to avoid numerical oscillations in the procedure of exchanging message, a damping factor λ is introduced, which is between 0 and 1. Each message is set to λ times its value from the previous iteration plus 1-λ times its prescribed updated value. For example, if the value of $a(i, k)$ by the message-passing procedure is $a(i, k)_{\text{cur}}$, the old value of $a(i, k)$ is $a(i, k)_{old}$, then the new value of $a(i, k)_{\text{new}}$ is $(1-\lambda) \times a(i, k)_{\text{cur}} + \lambda \times a(i, k)_{old}$.

In our experiments, we set dumping parameter λ as 0.5, initialize the $s(k, k)$ to be the minimum of the input similarity matrix and fix the cluster number to be 2.

Unlike other methods for which the number of clusters must be specified, and which are quite sensitive to the initial selection of centers, AP takes as input a real number $s(k, k)$ for each point k. Experiment done by B. J. Frey and D. Dueck has shown that AP finds clusters with much lower error. More details and proof about the AP algorithm can be found in [8].

B. K-means

The *K*-means [9] algorithm works as follows. Firstly, it randomly selects k of the objects, each of which initially represents a cluster mean. For each of the remaining objects, an object is assigned to the cluster to which is the most similar based on the distance between the object and the cluster mean. Then it computes the new mean of each cluster. This procedure iterates until the criterion function converges. The squared-error criterion is defined as expression (5):

$$E = \sum_{i=1}^{k} \sum_{p \in C_i} \left| p - m_i \right|^2 . \quad (5)$$

Where E is the sum of square-error for all objects in the database, p is the point in the space representing a given object, and m_i is the mean of cluster C_i. The algorithm attempts to determine k partitions that minimize the squared-error function.

From these two clustering algorithms, we can see that the classical *K*-means clustering result is related to its initial cluster means value while that of AP is not.

C. HSI Color Space

The difficulty of using the RGB color space is that it does not model the psychological understanding of color closely. The HSI model, which follows the human visual perception closely, is a better color model. This color model separates the color components in terms of chromatic and achromatic information [10].

The HSI model manipulates color images with the following transformation from the RGB model [9]:

$$\begin{bmatrix} I \\ V1 \\ V2 \end{bmatrix} = \begin{bmatrix} \frac{1}{3} & \frac{1}{3} & \frac{1}{3} \\ \frac{-\sqrt{6}}{6} & \frac{-\sqrt{6}}{6} & \frac{-\sqrt{6}}{6} \\ \frac{1}{\sqrt{6}} & \frac{-2}{\sqrt{6}} & 0 \end{bmatrix} \begin{bmatrix} R \\ G \\ B \end{bmatrix}, \quad (6)$$

$$S = \sqrt{(V_1^2 + V_2^2)}\ , \tag{7}$$

$$H = \tan^{-1}(\frac{V_2}{V_1})(if\ \mathrm{V}_1 \neq 0)\ . \tag{8}$$

Note that hue and saturation taken together are called chromaticity and the brightness of a chromatic light embodies the achromatic notion of intensity [11].

It has been observed that shadowed regions in HSI space hold the following properties [14] [15]:

1) Lower intensity: because the electro-magnetic radiance from the Sun is obstructed.

2) Higher saturation with short blue-violet wavelength: due to the atmospheric Rayleigh scattering effect.

3) Increased hue values: because the change of intensity of an area when shadowed and no-shadowed is positive proportional to the wavelength.

Once the image is converted from RGB color space to HSI color space, the aforementioned properties can be used to detect shadows.

III. METHODOLOGY

A. Clustering in HSI Color Space

In a sense, shadow detection can be treated as a problem of image segmentation, which is to separate an image into two regions. However, image segmentation can be viewed as a clustering process [6] [12] [16]. The goal of clustering is to group pixels together that exhibits some type of similarity such as color, texture, or brightness to form shadowed region and no-shadowed region. The clustering algorithm is based upon pixel similarity, and the location of boundaries between regions comes very naturally to the human observer [6].

We know that shadows hold large hue values; however, in colored remote sensing images, there are objects not shadowed with large hue values, such as blue buildings, rivers, grasslands, and so on, which should be distinguished out from shadows. For bluish objects, which always have high intensity values while shadows have low ones. Therefore, shadows could be described as regions with large hue values, low intensity values. However, there still exist objects not shadowed in colored remote sensing images with low intensity values, for example, the presence of water and high reflective regions, etc., we should remove them from shadows by using other characteristics of shadows, such as increased hue values and higher saturation. As a result, using a single band of data usually does not give us enough information to distinguish between shadows and other dark objects. Therefore, we employ a set of color invariant indices in order to discriminate between shadow regions and other dark areas in remote sensing images.

Following the analysis from above, we use the AP clustering algorithm to detect shadows by fusing the features of increased hue, high saturation, and lower luminance of the shadow region in the HSI color space.

When using AP, we should set similarity matrix first. In the hue space, we redefine the similarity $s(i, k)$ for points H_i and H_k as expression (9):

$$s(H_i, H_k) = \begin{cases} |H_i - H_k| & |H_i - H_k| \le \pi \\ 2\pi - |H_k - H_i| & |H_i - H_k| > \pi \end{cases}\ . \tag{9}$$

In the saturation and intensity space, similarity s(i, k) for points x_i and x_k is defined as expression (10):

$$s(i,k) = -\left\| x_i - x_k \right\|^2\ . \tag{10}$$

AP clustering method considers all data points as potential exemplars simultaneously at first.

As we known, raw pixel matrix for a given image usually is a large-scale matrix. If we apply AP algorithm directly on it, it will consume a large amount of system resources and spend a lot of time when calculate the similarity matrix. Therefore, before clustering, we can divide the image matrix into several blocks. We can divide matrix by row, column or blocks according to the requirements. Thus, the number of the sample points may be reduced and the efficiency of the algorithm will be improved a lot.

B. Fusion

Firstly, we calculate the histogram of the H component. By applying AP clustering, the centers of two classes H_{c1}, H_{c2} and the membership functions of the two classes are obtained [15]. Each pixel's grades of membership for each class can be given as expression (11):

$$\mu_{Hc1}(H(x,y))\mu_{Hc2}(H(x,y))\ , \tag{11}$$

$H(x, y)$ is the H component of the pixel at (x, y). These two values usually add up to 1.

Secondly, we deal with the S and I components using the same method as the H component respectively. Each pixel's grades of membership for each class can be expressed as expression (12) and (13):

$$\mu_{Sc1}(S(x,y))\mu_{Sc2}(S(x,y))\ , \tag{12}$$

$$\mu_{Ic1}(I(x,y))\mu_{Ic2}(I(x,y))\ . \tag{13}$$

Now we obtain six grades of membership for each pixel in the image. Since the pairs add up to 1. $\mu_{Hc1}(H(x, y))$, $\mu_{Sc1}(S(x, y))$ *and* $\mu_{Ic1}(I(x, y))$ are chosen to represent the overall color characteristics of the pixel. Fusing these three grades of membership to form a three-dimensional feature vector as expression (14):

$$C = (\mu_{Hc1}(H(x,y)), \mu_{Sc2}(S(x,y)), \mu_{Ic2}(I(x,y)))\ . \tag{14}$$

Finally, by applying the AP algorithm on the fused feature space, we obtain the final detection result for remote sensing images.

C. Algorithm Flow of the Proposed Method

The proposed method includes five major steps as follow:

1) Input a remote sensing image $F(x, y)$.

2) Space conversion from RGB color space into HSI space, and $F(x, y)$ is converted into $G(x, y)$.

3) The AP clustering algorithm is utilized to detect shadows in the H, S, and I components, respectively. Firstly, we divide the original images by column, then use AP to each column and obtain representative points of every column, and we can get the final clustering results by using AP to these representative points of every column. AP can group image pixels into any number of clusters. In our experiments, we choose the cluster number to be two, which are shadow region and no-shadowed region.

4) Three detected result images are fused to obtain a final shadow detection image $R_0(x, y)$. Concrete procedure of fusion has been discriped in subsection B of Section III.

5) Enhance outline of the shadow area by applying operations in mathematical morphology [20]. The purpose of this step is to eliminate any outlier and island pixel within the boundary of shadow. The operation steps as shown in expression (15):

$$R(x, y) = f_c(f_o(R_0(x, y), g), g) \tag{15}$$

where f_c denotes close operation, f_o denotes open operation, g denotes structural elements. The shape size of the structural elements is the key to remove isolated points to fill the empty area. For different images we need to utilize different structural elements.

In order to observe the effect of detection and compensate the information of shadow region later, we adopt a binary image which has the same size with the original image to identify the detection results. The pixel value which is zero on the binary image represents that the pixel belongs to shadow region; and the pixel value which is 255 on the binary image represents that the pixel belongs to no-shadowed region. The algorithm flow is shown in Fig. 1.

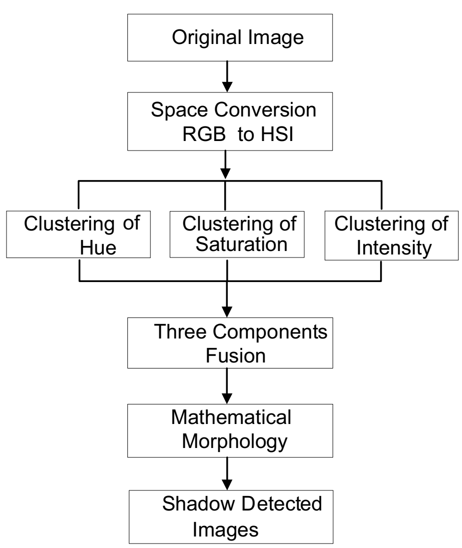

Figure 1. Flowchart of the proposed method

IV. EXPERIMENTAL RESULTS

In this experiment, we also compared *K*-means and histogram threshold method, which were implemented in MATLAB R2007a under Microsoft Windows XP environment. In the proposed method, in order to use the index value of the whole remote sensing image easily, we divide the image by column and apply AP for each column. Thus, we get the representative points of every column, than apply AP to these representative points. Through iterations, we get the final

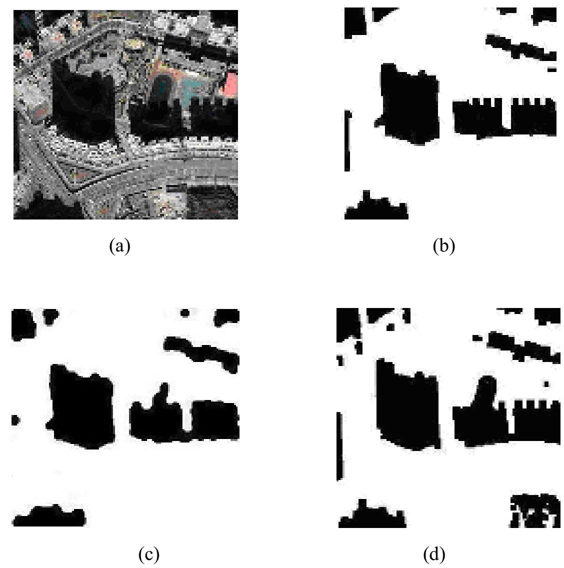

Figure 2. Shadow detection results for image one. (a) Original Image, (b) The proposed method, (c) *K*-means, and (d) Histogram threshold methods.

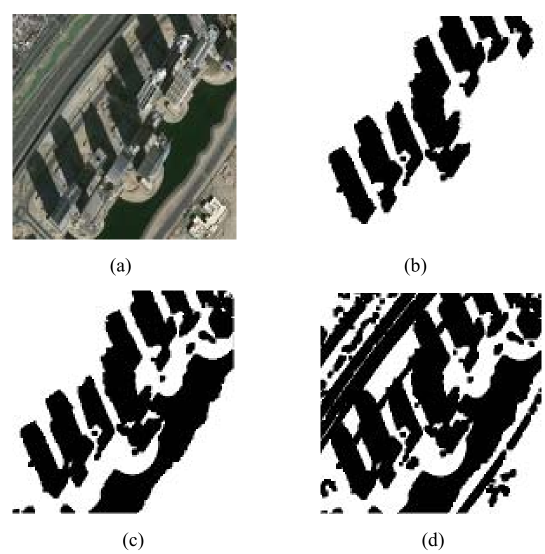

Figure 3. Shadow detection results for image two. (a) Original Image, (b) The proposed method, (c) *K*-means, and (d) Histogram threshold methods.

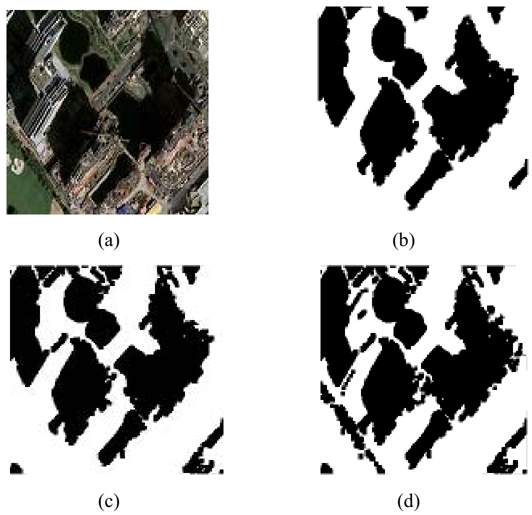

Figure 4. Shadow detection results for image three. (a) Original Image, (b) The proposed method, (c) *K*-means, and (d) Histogram threshold methods.

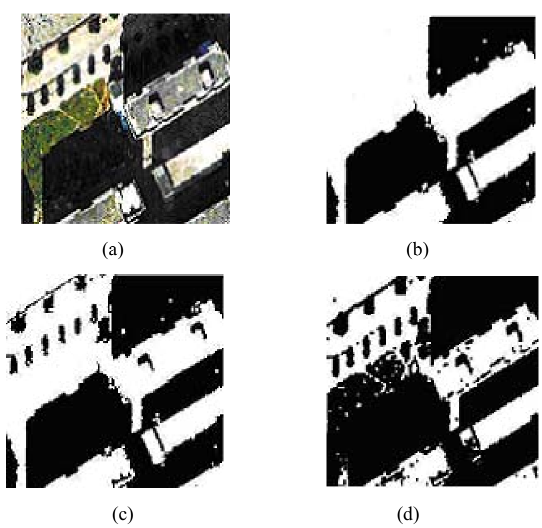

Figure 5. Shadow detection results for image four. (a) Original Image, (b) The proposed method, (c) K-means, and (d) Histogram threshold methods.

detection result. Experimental images with heavy shadows were downloaded from Google Earth. Four comparative experiment results for shadow detection are shown in Fig. 2, Fig. 3, Fig. 4 and Fig. 5 respectively. Since images used in the experiments are real remote sensing images downloaded from Google Earth, we cannot evaluate the algorithm performance by objective numerical values because lack of criterion. Here the only way to evaluate the algorithm performance is by comparing the visual effects.

In these figures, the original color remote sensing images are shown in subfigure (a). Subfigure (b) is the result of applying the AP clustering in the HSI color space; Subfigure (c) shows the result using *K*-means; and subfigure (d) is the detection result using histogram threshold method [5]. Fig. 2 is a remote sensing image with heavy shadowed building, high reflective regions, and dark green lawn. We observe that the proposed method solves the problems of false dismissals, and it improves the accuracy of shadow detection. Fig. 3 demonstrates a quite different example with dark road and blue water which also exhibit higher hue and lower luminance as the same as shadow regions. It is easy to see that the proposed method can obtain the shadow regions more precisely.

Fig. 4 and Fig. 5 are typical examples with the presence of water area, dark green lawn and high reflective regions, which have the similar hue with shadow region. We also observe that the proposed method can exclude water area from shadows as well.

The comparison results show that the proposed method can distinguish dark objects from shadows, and the shape of the segmented shadows is preserved well, it has a higher detection precision than that of *K*-means and histogram threshold method. For *K*-means, the clustering result is related to its initial cluster mean value, while that of AP is not. Threshold method is mainly suitable for gray images. Meanwhile, there is no universal method to determine threshold for all images. Besides, repeated experiments show that the proposed method has better stability than *K*-means.

As for the execution speed of the proposed method, it is not optimized in this work. The computational complexity of AP is $O(N^2)$, while those of *K*-means and threshold method both are $O(N)$. To speed up the algorithm, one of the solutions is to take the strategy of "divide and conquer". In the experiments, when we divide the image feature matrix into several blocks, the number of the sample points may be reduced in each block and the efficiency of the algorithm will be improved a lot. In particular, we divide the original images by column, and the size of the images used in our experiment is 128×128. In AP algorithm, we set dumping parameter λ to be 0.5, the cluster number to be 2, and fixed the number of iterations is 3. Table I shows runtime of different methods for image F1, F2, F3, and F4, time unit is in Second. The time shown in table refers to the average runtime after implementing four times clustering.

Although the execution speed of AP is not optimal, it has higher detection precision than other clustering algorithms, such as *K*-means or threshold method. The higher detection accuracy and better stability proved that the proposed method can be well applied to shadow detection for remote sensing images when there is lack of prior knowledge. Besides, detection procedure does not require manual intervention.

TABLE I. RUN TIME OF DIFFERENT ALGORITHMS

	AP	***K*-means**	**Threshold**
Image F1	120.08	45.12	1.19
Image F2	126.82	48.37	1.38
Image F3	117.97	39.88	0.97
Image F4	119.61	42.46	1.03

V. CONCLUSIONS AND FUTURE WORKS

In this paper, we analyzed the shadow properties in HSI color space, and presented an efficient method to detect shadows for remote sensing images, which using AP clustering algorithm and fusing the detected results in the H, S and I components. Test images contain the areas which are mainly heavy shadowed buildings.

The proposed method to detect shadow of remote sensing images as presented here mainly concerned about the similarity between colors. Further study is to find a better similarity measure when using AP clustering algorithm. Two aspects of spatial information and color components will be taken into consideration. It is the fact that AP can automatically choose the clusters number if we do not manually fix it. However, whether the two clusters are suitable to the application of color image segmentation is an interesting problem. For example, if there are various regions in remote sensing images with heavy shadows, which are similar to shadowed region, how to group them into shadowed region and no-shadowed region automatically without fixing the cluster number beforehand should be investigated.

ACKNOWLEDGMENT

The research work described in this paper was fully supported by the grants from the National Natural Science Foundation of China (Project No. 60675011, 90820010). Prof. Ping Guo is the author to whom the correspondence should be addressed, his e-mail address is pguo@ieee.org.

REFERENCES

[1] E. Salvador, A. Cavallaro, and T. Ebrahimi, "Cast shadow segmentation using invariant color features," Computer Vision and Image Understanding, vol. 95, no. 2, pp. 238-259, 2004.

[2] E. Salvador, A. Cavallaro and T. Ebrahimi, "Shadow identification and cassification using invariant color models," Proceedings of the IEEE International Conference on Acoustics, Speech and Signal Processing, vol. 3, pp. 1545-1548, 2001.

[3] G. D. Finlayson, S. D. Hordley, C. Lu, and M. S. Drew, "On the removal of shadows from images," IEEE Trans. on Pattern Analysis and Machine Intelligence, vol. 28, no. 1, pp. 59-68, 2006.

[4] J. L. Wang, "The research of shadow detection algorithms based on color aerial images," M.S. thesis, Department of Remote Sensing Information Engineering, Wuhan University, Wuhan, China, 2005 (in Chinese).

[5] F. C. Cheng, Y. K. Chen, and K. T. Liu, "An efficient gray-level clustering algorithm for image segmentation," Proceedings of the IEEE International Conference on Informatics in Control, Automation and Robotics, vol. 2, no. 6, pp. 259-262, 2009.

[6] A. Weeks and G. Eric Hague, "Color segmentation in the HSI color space using the K-means algorithm," Proceedings of SPIE Symposium on Electronic Imaging, vol. 3026, pp. 143-154, 1997.

[7] S. U. Lee, S. Y. Chung and R. H. Park, "A comparative performance study of several global thresholding techniques for segmentation," Computer Vision, Graphics and Image Processing, vol. 52, no. 2, pp. 171-190, 1990.

[8] B. J. Frey and D. Dueck, "Clustering by Passing Messages between data points," Science, vol. 315, no. 5814, pp. 972-976, 2007.

[9] T. Kanungo, D. M. Mount, and N. S. Netanyahu, "An efficient K-means clustering algorithm: analysis and implementation," IEEE Trans. on Pattern Analysis and Machine Intelliqence, vol. 24, no. 7, pp. 881-892, 2002.

[10] Victor J. D. Tsai, "A comparative study on shadow compensation of color aerial images in invariant color models," IEEE Trans. on Geoscience and Remote Sensing, vol. 44, no. 6, pp.1661-1671, 2006.

[11] J. Huang, W. Xie and L. Tang, "Detection of and compensation for shadows in colored urban aerial images," Proceedings of the 5th Word Congr. Intelligent Control and Automation, vol. 4, pp. 3098-3100, 2004.

[12] P. Guo and Lyu MR, "A study on space selection for determining image segmentation region number," Proceedings of International Conference on Artificial Inteligence, vol. 1, no. 3, pp.1127-1132, 2000.

[13] J. Yao and Z. F. Zhang. "Hierarchical shadow detection for color aerial images," Computer Vision and Image Understanding, vol. 102, no. 1, pp. 60-69, 2006.

[14] V. Arévalo, J. González, and G. Ambrosio, "Shadow detection in colour high-resolution satellite images," International Journal of Remote Sensing, vol. 29, no. 7, pp. 1945-1963, 2008.

[15] J. Yang and Z. M. Zhao, "A shadow removal method for high resolution Remote Sensing image," Journal of Wuhan University (Information Science). vol. 33, no. 1, pp.17-20, 2008(in Chinese).

[16] B. Rao, G. Zheng, T. M. Chen, J. Huang, and X. Shao, "An efficient hierarchical method for image shadow detection," Proceedings of 2nd International Workshop on Knowledge Discovery Date Mining, vol. 2, no. 2, pp. 622-627, 2009.

[17] W. Zhang, F. X. Zang, and X. K. Yang, "Moving cast shadows detection using ratio edge," IEEE Trans. on Multimedia, vol. 9, no. 6, pp. 1202-1214, 2007.

[18] P. Guo and H. Q. Lu, "A study on Bayesian Probabilistic image automatic segmentation," Acta Optica Sinica, vol. 22, no. 12, pp. 1479-1483, 2002 (in Chinese).

[19] K. L. Chung, Y. R. Lin, and Y. H. Huang, "Efficient shadow detection of color aerial images based on successive thresholding scheme," IEEE Trans. On Geoscience and Remote Sensing, vol. 47, no. 2, pp. 671-682, 2009.

[20] S. Nomura, K. Yamanaka, T. Shiose, H. Kawakami, and O. Katai, "Morphological preprocessing method to thresholding degraded word image," Pattern Recognition Letters, vol. 30, no. 8, pp. 729-744, 2009.

[21] J. H. Guo, P. Gong, and L. Liang, "Removing shadows from Google Earth satellite images," Proceedings of SPIE, vol. 6752, no. 2, pp. 1-12, 2007.